

# Luminescence from highly excited nanorings: Luttinger liquid description

T. V. Shahbazyan

*Department of Physics and Astronomy, Vanderbilt University, Nashville, TN 37235*

I. E. Perakis\*

*Department of Physics, University of Crete, P.O. Box 2208, 710 03, Heraklion, Crete, Greece*

M. E. Raikh

*Department of Physics, University of Utah, Salt Lake City, UT 84112*

We study theoretically the luminescence from quantum dots of a ring geometry. For high excitation intensities, photoexcited electrons and holes form Fermi seas. Close to the emission threshold, the single-particle spectral lines acquire weak many-body satellites. However, away from the threshold, the discrete luminescence spectrum is completely dominated by many-body transitions. We employ the Luttinger liquid approach to *exactly* calculate the intensities of *all* many-body spectral lines. We find that the transition from single-particle to many-body structure of the emission spectrum is governed by a single parameter and that the distribution of peaks away from the threshold is *universal*.

PACS numbers: 71.10.Ca, 71.45.-d, 78.20.Bh, 78.47.+p

## I. INTRODUCTION

Photoluminescence (PL) from zero-dimensional objects (quantum dots) is one of the highlights in physics of nanostructures which emerged during the last decade. Early papers (see, e.g., Refs. 1,2, and the review article Ref. 3) reported the PL spectra consisting of "zero-width" luminescence lines. High surface density of quantum dots caused an ambiguity in assigning of these lines. In the later studies the emission from a *single* dot was resolved. This progress<sup>4</sup> has permitted the PL spectroscopy of individual dots with controllable exciton population determined by the excitation intensity, and also at tunable charge states.<sup>5,6</sup>

At low excitation intensity the number of excitons in a dot is either one or zero. Then the emission line corresponds to the transition between the lowest size-quantization levels in the conduction and the valence bands. Upon increasing the excitation intensity, the number of excitons in a dot,  $N$ , can be larger than one. This leads to the features in the PL spectrum which must be interpreted in terms of recombination within many-exciton complexes.<sup>7-16</sup> Different recombination processes within a complex result in a multitude of the emission lines. One reason for an emergence of additional PL lines is that, for  $N > 2$ , the carriers constituting the complex occupy higher size-quantization levels. Another reason, is that the interactions between the strongly confined photoexcited carriers lift the *de-*

*generacies* of the final many-body states. The latter mechanism of interaction-induced multiplication of the emission lines was addressed in Refs. 11,12,17 for the situations with<sup>17</sup> and without<sup>11,12</sup> orbital degeneracy of single-particle states. The calculations carried out in Refs. 11,12,17 predicted the splittings of the PL lines, originating from different many-body final states, to be of the order of the matrix element of the interaction potential. The actual positions of the lines predicted by these calculations reproduce quite accurately the experimental PL spectra of Refs. 11-14 (for up to  $N = 16$ ) and of Ref. 16 (for  $1 \leq N \leq 6$ ).

Within the approaches of Refs. 11,12,17, each many-body line corresponds to recombination of an electron and a hole having the *same* size-quantization quantum numbers. We note here that in the experiment<sup>11,12</sup> additional emission lines have been observed that were identified with the transitions between *different* size-quantization levels. These transitions originate from a *shake-up* effect in a confined electron-hole system. Namely, the radiative recombination of an electron-hole pair is accompanied by an *internal* excitation within the exciton multiplex. These many-body processes are missed within the theoretical approaches of Refs. 11,12,17. Meanwhile, as we argue below, the PL lines originating from the shake-up processes multiply very rapidly with increasing  $N$ , and for high enough  $N$  become the dominant feature of the PL spectrum. Here we develop a theory of the many-body luminescence from a quantum dot for the limiting case  $N \gg 1$ .

When a number of photoexcited carriers is large, an adequate description of PL from a dot must be developed in terms of Fermi seas formed by equal numbers (determined by excitation) of electrons and holes in conduction and valence bands, respectively (see inset in Fig. 1). As in the case of a small number of carriers, such a description is based on the fact that PL is preceded by a fast nonradiative relaxation of electrons and holes into the corresponding ground states.<sup>11-16</sup> Microscopic mechanism of this relaxation is addressed, e.g., in Ref. 18.

For noninteracting system, the emission lines would correspond to transitions between size-quantization levels in conduction and valence bands which obey the selection rules. Within this description, the single-particle

emission spectrum near the Fermi edge is given by the Golden rule,

$$I(\omega) \propto \sum_n C_n \delta[\omega + (\Delta_1 + \Delta_2)n], \quad (1)$$

where  $\Delta_1$  and  $\Delta_2$  are level spacings for electrons and holes;  $C_n$  are the oscillator strength which depend on  $n$  only *weakly* ( $\omega < 0$  is measured from the Fermi edge).

As discussed above, the many-body transitions, resulting from interactions of carriers in a dot, change *qualitatively* the form of the spectrum. Analogously to recombination within an exciton multiplex, here a removal of an e-h pair shakes up the respective Fermi seas by causing them to emit Fermi sea excitations. Since in a *finite* system, the energies of excitations are *quantized*, such a shake-up would lead to the spectrum of a form

$$I(\omega) \propto \sum_{mn} C_{mn} \delta(\omega + m\tilde{\Delta}_1 + n\tilde{\Delta}_2), \quad (2)$$

rather than Eq. (1). Here  $\tilde{\Delta}_1$  and  $\tilde{\Delta}_2$  are the level spacings renormalized by interactions. All the information about many-body correlations in the system is encoded in the oscillator strengths  $C_{mn}$ . As we will see below,  $C_{mn}$ , being governed by interactions, are *strong functions* of  $m$  and  $n$ .

The goal of the present paper is to demonstrate that the oscillator strengths  $C_{mn}$  can be evaluated *analytically* for a dot of a ring geometry. Such dots have been recently fabricated<sup>5</sup> and their emission spectra (including many-body effects) were studied for low excitation intensities both experimentally<sup>19,20</sup> and theoretically.<sup>21–26</sup> Our approach is valid when the number of carriers,  $N$ , is large enough (the accuracy is  $1/N$ ). However, this "asymptotic" consideration allows us to establish the *universal* properties of the many-body spectrum away from the threshold.

For a ring-shaped dot, the electron and hole Fermi seas represent one-dimensional (1D) systems. This allows us to use the finite-size Luttinger-liquid description<sup>27</sup> for calculation of the emission spectrum. Note that the Luttinger liquid model was employed earlier for calculations of the Fermi-edge optical properties of *infinite* 1D systems (with and without defects) in Refs. 28–32.

We show that due to a finite size of the system, the structure of the emission spectrum is different in low- and high- $\omega$  domains. Namely, for  $\mu \ln|\omega/(\tilde{\Delta}_1 + \tilde{\Delta}_2)| \ll 1$  (low frequencies) the spectrum is dominated by single-particle peaks; many-body satellites have a relative magnitude  $\sim \mu$ , where  $\mu \ll 1$  is the dimensionless interaction strength (Luttinger liquid parameter). For high frequencies (i.e.,  $\mu \ln|\omega/(\tilde{\Delta}_1 + \tilde{\Delta}_2)| \gg 1$ ), the many-body peaks *completely dominate* the spectrum; roughly speaking, in the high- $\omega$  domain, the oscillator strengths of single-particle peaks are evenly distributed among the multitude of many-body peaks. Furthermore, the peaks cluster into groups (generations), so that the patterns

of peaks within the neighboring generations are almost identical.

## II. EMISSION FROM A LUTTINGER LIQUID RING

We start with the two-component Luttinger liquid model on a ring<sup>36</sup> with Hamiltonian  $H_1 + H_2 + H_{int}$ , where  $H_j$  describe noninteracting electrons ( $j = 1$ ) and holes ( $j = 2$ ) with linearized dispersions (the slopes are determined by the Fermi velocities  $v_j$ );  $H_{int}$  describes the interactions between carriers via screened potential  $U(x)$ . The e-h recombination rate is given by the Golden rule

$$\begin{aligned} W(\omega) &= \frac{2\pi}{L} \sum_f |\langle f|T|i \rangle|^2 \delta(E_i - E_f - \omega) \\ &= \frac{1}{L} \int_{-\infty}^{\infty} dt e^{-i\omega t} \langle i|T^\dagger(t)T(0)|i \rangle, \end{aligned} \quad (3)$$

where  $E_i$  and  $E_f$  are the energies of initial (ground) and final (with e-h pair removed) states, and

$$T = T_+ + T_- \quad T_\pm = d \int_0^L dx \psi_{2\mp}(x) \psi_{1\pm}(x) \quad (4)$$

is the dipole transition operator. Here  $\psi_{i\pm}$  are annihilation operators for left ( $-$ ) and right ( $+$ ) moving carriers,  $d$  is the interband dipole matrix element, and  $L$  is the ring circumference. Note that recombination occurs between left (right) electrons and right (left) holes. The recombination rate is then expressed via a four-particle Green function,

$$\begin{aligned} W(\omega) &= d^2 \int_0^L dx \int_{-\infty}^{\infty} dt e^{-i\omega t} [D_+(x, t) + D_-(x, t)] \\ &= d^2 [D_+(\omega) + D_-(\omega)], \\ D_\pm(x, t) &= \langle \psi_{2\mp}^\dagger(x, t) \psi_{1\pm}^\dagger(x, t) \psi_{1\pm}(0) \psi_{2\mp}(0) \rangle. \end{aligned} \quad (5)$$

In order to evaluate  $D_\pm(x, t)$  for a two-component Luttinger liquid,<sup>33–35</sup> we use the bosonization technique on a ring<sup>36</sup> (see Appendix A). The final result reads

$$\begin{aligned} D_\pm(x, t) &= \frac{e^{-it\delta_P}}{L^2} \epsilon^{2(\mu_2 + \mu_2)} \\ &\quad \times \left[ f_\pm(z_{1\pm}) \right]^{1+\mu_1} \left[ f_\mp(z_{1\mp}) \right]^{\mu_1} \\ &\quad \times \left[ f_\mp(z_{2\mp}) \right]^{1+\mu_2} \left[ f_\pm(z_{2\pm}) \right]^{\mu_2}, \end{aligned} \quad (6)$$

where  $\delta_P = \pi(v_1 + v_2)/L$  is the energy shift (to be absorbed into the frequency) due the change in the parity of electron and hole numbers, and  $\epsilon$  is a cutoff. The coordinate dependence of  $D_\alpha(x, t)$  is determined by ( $\alpha = \pm$ )

$$f_\alpha(z_{j\alpha}) = \frac{1}{1 - e^{i\alpha(2\pi z_{j\alpha}/L + \alpha i\epsilon)}}, \quad z_{j\alpha} = x - \alpha \tilde{v}_j t. \quad (7)$$

The explicit expressions for renormalized Fermi velocities  $\tilde{v}_j$  and interaction-induced exponents  $\mu_j$  are given in Appendix A. Correspondingly, the level spacings are now  $\tilde{\Delta}_j = 2\pi\tilde{v}_j/L$ . The interaction strength is characterized by the ratio  $u/v_j$ , with

$$u = \frac{1}{\hbar\pi} \int dx U(x) \quad (8)$$

being the Fourier of screened potential; this ratio represents the average (screened) interaction in units of the (bare) level spacing near the Fermi energy. For weak interactions,  $u/v_j \ll 1$ , we have (see Appendix A)

$$\mu_j \simeq (u/4v_j)^2, \quad \tilde{\Delta}_j \simeq \Delta_j(1 + u/2v_j). \quad (9)$$

The correlator  $D_\alpha(x, t)$  is periodic in variables  $z_{j\alpha}$ . In order to carry out the integration in Eq. (5) we first perform the Fourier expansion of  $[f_\alpha(z_{j\alpha})]^\nu$  as

$$[f_\pm(z_{j\pm})]^\nu = \frac{\sin \pi\nu}{\pi} \sum_n B(n + \nu, 1 - \nu) e^{\pm 2\pi i n z_{j\pm}/L}, \quad (10)$$

where  $B(x, y)$  is the Beta-function. Substituting this expansion into Eq. (6), and then into Eq. (5), we arrive at the expected form Eq. (2) of the emission spectrum with the coefficients  $C_{mn}$  cast in the following closed form (see appendix B).

$$C_{mn} = \int_{-\pi}^{\pi} \frac{d\phi_1 d\phi_2 d\phi_3}{(2\pi)^3} \frac{\epsilon^{2(\mu_1+\mu_2)} e^{-\frac{i}{2}(\phi_1+\phi_2)(m+n)}}{(1 - e^{i\phi_1})^{1+\mu_1} (1 - e^{i\phi_2})^{1+\mu_2}} \times \frac{e^{-\frac{i}{2}\phi_3(m-n)}}{(1 - e^{i(\phi_2-\phi_3)})^{\mu_1} (1 - e^{i(\phi_1+\phi_3)})^{\mu_2}}. \quad (11)$$

Note, that the sum in Eq. (2) is constrained by the selection rule that  $m$  and  $n$  are of the same parity, i.e., the combinations

$$N = (m + n)/2, \quad M = (m - n)/2, \quad (12)$$

which enter into the rhs of Eq. (11), are integers. This is the result of the linear dispersion of electrons and holes near the Fermi levels.

Formula (11) for the oscillator strengths is the main result of this section. It is easy to see that it correctly reproduces the non-interacting limit. Indeed, upon setting  $\mu_i = 0$ , the integral over  $\phi_3$  yields  $C_{mn} = \delta_{mn}$ . Another important limiting case  $m, n \gg 1$  corresponds to the transitions well away from the Fermi edge. In this case, the main contribution to the integral (11) comes from the domain  $\phi_1 + \phi_2 \sim (m + n)^{-1} \ll 1$ . Within this domain, one can neglect the difference between  $\phi_1$  and  $-\phi_2$  in the last two factors in the denominator. Then the integrals over  $\phi_1, \phi_2$  factorize, yielding

$$C_{mn} = \frac{\Gamma(N + 1 + \mu_1)\Gamma(N + 1 + \mu_2)}{\Gamma(1 + \mu_1)\Gamma(1 + \mu_2)[\Gamma(N + 1)]^2} K(M), \quad (13)$$

with

$$K(M) = \int_{-\pi}^{\pi} \frac{d\phi}{2\pi} \frac{\epsilon^{2(\mu_1+\mu_2)} e^{iM\phi}}{(1 - e^{-i\phi})^{\mu_1} (1 - e^{i\phi})^{\mu_2}} = \frac{\epsilon^{2(\mu_1+\mu_2)} (-1)^M \Gamma(1 - \mu_1 - \mu_2)}{\Gamma(1 - M - \mu_1)\Gamma(1 + M - \mu_2)}, \quad (14)$$

where  $\Gamma(x)$  is the Gamma-function. It can be seen from Eq. (14) that, for a given  $N$ , the oscillator strengths,  $C_{mn}$ , fall off as  $C_{mn} \propto |M|^{\mu_1+\mu_2-1}$  with increasing  $|M| = \frac{1}{2}|m - n|$ . This slow power-law decay reveals strong correlations within electron-hole system on a ring. Finally, using the large  $x$  asymptotics of  $\Gamma(x)$ , we obtain the expression for the oscillator strengths valid for  $N, |M| \gg 1$ ,

$$C_{mn} = \frac{\epsilon^{2\mu}\Gamma(1 - \mu)}{\Gamma(1 + \mu_1)\Gamma(1 + \mu_2)} \frac{\sin \pi\tilde{\mu}}{\pi} N^\mu |M|^{\mu-1}, \quad (15)$$

where  $\mu = \mu_1 + \mu_2$ , and  $\tilde{\mu} = \frac{1}{2}\mu + \frac{1}{2}(\mu_1 - \mu_2)\text{sgn}M$ .

### III. MANY-BODY STRUCTURE OF THE EMISSION SPECTRUM

The general expression (11) determines the heights of the emission peaks, while the *order* of the peaks with different  $\{m, n\}$  is governed by the  $\delta$ -functions in Eq. (2), which ensure the energy conservation. Therefore, this order depends crucially on the relation between  $\tilde{\Delta}_1$  and  $\tilde{\Delta}_2$ . Moreover, a *commensurability* between  $\tilde{\Delta}_1$  and  $\tilde{\Delta}_2$  leads to accidental degeneracies in the positions of the emission lines. However, in order to establish the general properties of the spectrum, it is instructive to consider first two particular cases of commensurate  $\tilde{\Delta}_1$  and  $\tilde{\Delta}_2$ .

We start with the symmetric case  $\tilde{\Delta}_i = \tilde{\Delta}/2$  (and, hence,  $\mu_i = \mu/2$ ). The peak positions, as determined by Eq. (2), coincide with those for single-particle transitions,  $|\omega| = N\tilde{\Delta}$ . The corresponding oscillator strengths can be straightforwardly evaluated from Eq. (11) as

$$c_N = \sum_M C_{N+M, N-M} = \left[ \int_{-\pi}^{\pi} \frac{d\phi}{2\pi} \frac{\epsilon^\mu e^{-iN\phi}}{(1 - e^{i\phi})^{1+2\mu}} \right]^2. \quad (16)$$

For  $N \gg 1$ , the denominator of the integrand can be expanded, yielding

$$c_N \simeq (\epsilon N)^{2\mu} = \left| \frac{\epsilon\omega}{\tilde{\Delta}} \right|^{2\mu}. \quad (17)$$

Note that single-particle oscillator strengths correspond to  $c_N = 1$ . We thus conclude that interactions affect strongly the peak heights for  $|\omega/\tilde{\Delta}|^{2\mu} \gg 1$ , i.e.,

in the high frequency domain. In fact, even for an arbitrary relation between  $\tilde{\Delta}_1$  and  $\tilde{\Delta}_2$ , the crossover between “single-particle” and “many-body” domains of the spectrum is governed by the dimensionless parameter  $\mu \ln|\omega/(\tilde{\Delta}_1 + \tilde{\Delta}_2)|$ .

Indeed, consider now the case  $\tilde{\Delta}_1 = 3\tilde{\Delta}_2$  (and thus  $\mu_2 \simeq 9\mu_1$ ) which renders a spectrum richer than (1) and (17). As follows from Eq. (2), the spectral positions of the peaks are given by  $|\omega|/(\tilde{\Delta}_1 + \tilde{\Delta}_2) = l/2$ , where  $l$  is an integer. The corresponding oscillator strengths can be evaluated explicitly from Eq. (11) (see appendix C). The final result reads

$$D_{\pm}(\omega) = \frac{2\pi}{L} \left| \frac{\epsilon\omega}{\tilde{\Delta}} \right|^{2\mu} \sum_l \left[ \frac{1 + \left| \frac{2\omega}{\tilde{\Delta}} \right|^{-\mu}}{2} \delta(\omega + \tilde{\Delta}l) + \frac{1 - \left| \frac{2\omega}{\tilde{\Delta}} \right|^{-\mu}}{2} \delta\left[\omega + \tilde{\Delta}(l + 1/2)\right] \right], \quad (18)$$

with  $\mu = \mu_1 + \mu_2 \simeq 10\mu_1$  and  $\tilde{\Delta} = \tilde{\Delta}_1 + \tilde{\Delta}_2 = 4\tilde{\Delta}_1$ .

The above result illustrates how the structure of the spectrum evolves as the frequency departs from the Fermi edge. For  $\mu \ln|\frac{\omega}{\tilde{\Delta}}| \ll 1$ , each single-particle peak,  $|\omega| = l\tilde{\Delta}$  acquires a weak many-body satellite at  $|\omega| = (l + \frac{1}{2})\tilde{\Delta}$ . In the opposite limit,  $\mu \ln|\frac{\omega}{\tilde{\Delta}}| \gg 1$ , the oscillator strength of an “integer” peak gets equally redistributed between the components of the doublet. The crossover frequency,  $\Omega$ , separating the “single-particle” and the developed many-body domains of the spectrum is determined by the condition  $\ln|\frac{\Omega}{\tilde{\Delta}}| \sim \mu^{-1}$ . The spectrum (18) is schematically depicted in Fig. 1.

Let us turn to the structure of the spectrum in the general case of incommensurate  $\tilde{\Delta}_1$  and  $\tilde{\Delta}_2$ . We start from the observation that the peak positions can be classified by “generations”. Namely, once a peak  $\{m, 0\}$  (or  $\{0, n\}$ ) emerges at  $\omega = \omega_m = -m\tilde{\Delta}_1$  (or  $\omega = \omega_n = -n\tilde{\Delta}_2$ ), it is followed by next generations of peaks  $\omega_m^{(k)} = \omega_m - k(\tilde{\Delta}_1 + \tilde{\Delta}_2)$  or  $\omega_n^{(k)} = \omega_n - k(\tilde{\Delta}_1 + \tilde{\Delta}_2)$  repeating with a period  $\tilde{\Delta} = \tilde{\Delta}_1 + \tilde{\Delta}_2$ . Thus, for a crude description of the spectrum away from the Fermi edge it is convenient to divide the frequency region  $\omega < 0$  into the intervals of width  $\tilde{\Delta}$ .

The number of peaks within the spectral interval  $\{-|\omega|, -|\omega| - \tilde{\Delta}\}$  is the number of integers satisfying the conditions  $|\omega| < m\tilde{\Delta}_1 + n\tilde{\Delta}_2 < |\omega| + \tilde{\Delta}$ . This number is equal to

$$\mathcal{N}_{\omega} = \frac{|\omega|\tilde{\Delta}}{2\tilde{\Delta}_1\tilde{\Delta}_2}, \quad (19)$$

where we assumed  $|\omega| \gg \tilde{\Delta}$  and took into account the parity restriction. From Eq. (19) we find the peak density  $g_{\omega} = \mathcal{N}_{\omega}/\tilde{\Delta} = |\omega|/2\tilde{\Delta}_1\tilde{\Delta}_2$ . It also follows from (19) that  $\mathcal{N}_{\omega-\tilde{\Delta}} - \mathcal{N}_{\omega} = \tilde{\Delta}^2/2\tilde{\Delta}_1\tilde{\Delta}_2$  generations start within each interval. Since the heights of consecutive peaks within

the interval  $\tilde{\Delta}$  vary non-monotonically, it is natural to characterize these heights by the distribution function

$$F(\mathcal{C}) = \frac{1}{2g_{\omega}} \int_0^{\infty} dm dn \delta(\omega + m\tilde{\Delta}_1 + n\tilde{\Delta}_2) \delta(C_{mn} - \mathcal{C}), \quad (20)$$

where  $C_{mn}$  is given by Eq. (15). Here we made use of the fact that  $\mathcal{N}_{\omega} \gg 1$  by treating  $m$  and  $n$  as continuous variables. The prefactor in Eq. (20) ensures the normalization ( $\int_0^{\infty} d\mathcal{C} F(\mathcal{C}) = 1$ ). It is easy to see that  $F(\mathcal{C})$  is nonzero in the interval between  $C_{min} = \min\{2\mu_{1,2}|\frac{\tilde{\Delta}_{1,2}}{\omega}|^{1-2\mu}\}$  and  $C_{max} = 2|\frac{\omega}{\tilde{\Delta}}|^{\mu} \max\{\mu_{1,2}\}$  (we omit the overall factor  $\epsilon^{2\mu}$ ). Within this wide interval,  $F(\mathcal{C})$  falls off as  $(\mathcal{C}_0/\mathcal{C})^{2+\mu}$ , where

$$\mathcal{C}_0 = \mu \left| \frac{\omega}{4} (\tilde{\Delta}_1^{-1} + \tilde{\Delta}_2^{-1}) \right|^{2\mu-1} \quad (21)$$

is the *typical* value of the oscillator strength. On the other hand, the *average* oscillator strength, which can be easily calculated from Eq. (20), is equal to  $\bar{\mathcal{C}} = \mu^{-1}\mathcal{C}_0 \gg \mathcal{C}_0$ . The distribution function  $F(\mathcal{C})$  is schematically depicted in Fig. 2. The fact that  $\bar{\mathcal{C}}$  *decreases* with  $|\omega|$  can be understood in the following way. As it is seen from Eq. (17), in the symmetric case, with only a single peak per interval  $\tilde{\Delta}$ , the peak heights increase with  $|\omega|$  as  $|\frac{\omega}{\tilde{\Delta}}|^{2\mu}$ . In the general case, this spectral intensity gets redistributed between  $\mathcal{N}_{\omega}$  different peaks. Thus,

$$\bar{\mathcal{C}} \sim \mathcal{N}_{\omega}^{-1} \left| \frac{\omega}{\tilde{\Delta}} \right|^{2\mu} \propto |\omega|^{2\mu-1}. \quad (22)$$

#### IV. CONCLUSIONS

In the present paper we derived the emission spectrum from a highly excited ring-shaped quantum dot. In this system electron-electron, hole-hole and electron-hole interactions relax the momentum conservation leading to a multitude of discrete emission lines. Luttinger liquid model employed in our calculation allows to evaluate the overlap integrals between the correlated initial and final many-body states. These overlap integrals determine the intensity of the corresponding spectral lines.

The theoretical value of the dimensionless interaction parameter  $\mu$  is determined by the ratio of screened interaction  $U$  to the level spacings  $\tilde{\Delta}_1$  and  $\tilde{\Delta}_2$  at the corresponding Fermi levels. Both quantities depend on the number of excited carriers,  $N$ , which in turn is determined by the excitation intensity. This, and the sensitivity of the screening to the details of experimental setup, lead to a common ambiguity in the theoretical determination of  $\mu$ . For example, in quantum wires, the value of  $\mu$  measured in resonant tunneling experiments,<sup>37,38</sup> was

significantly larger than theoretical estimates. Concerning the estimates for  $\tilde{\Delta}_1$  and  $\tilde{\Delta}_2$ , in the experimental paper Ref. 5 on luminescence from ring-shape dots, the total energy separation  $\tilde{\Delta}$  between the lowest level was approximately 5 meV. This value comes almost exclusively from the conduction band, due to the large ratio of the electron and hole effective masses. Both  $\tilde{\Delta}_1$  and  $\tilde{\Delta}_2$  increase linearly with increasing  $N$ . This implies that the shake-up processes within the hole system are experimentally much more relevant than those for electrons.

Note finally, that for emission from a finite electron-hole 1D system considered here, the physics underlying the interaction-induced multiplication of the number of lines with departure from the Fermi level is analogous to that for tunneling into a disordered quantum dot.<sup>39</sup>

## ACKNOWLEDGMENTS

Discussions with E. Ehrenfreund and D. Gershoni are gratefully acknowledged. The work at Vanderbilt was supported by ONR Grant No. N00140010951. The work in Utah was supported by NSF Grant No. INT-0003710, the Petroleum Research Fund under ACS-PRF Grant No. 34302-AC6, and by the Army Research Office under Grant No. DAAD 19-0010406.

## APPENDIX A:

Here we outline the calculation of the Green function (6) using a bosonisation scheme for the multicomponent Luttinger liquid on a ring.<sup>36</sup> The right/left fermion fields are presented as

$$\psi_{j\alpha}(x) = (2\pi\epsilon)^{-1/2} e^{i\varphi_{j\alpha}(x) + i\alpha\pi x/L}, \quad (\text{A1})$$

where right/left ( $\alpha = \pm$ ) bosonic fields  $\varphi_{j\alpha}(x)$  are related to the corresponding densities as  $\rho_{j\alpha}(x) = \frac{\alpha}{2\pi} \frac{\partial \varphi_{j\alpha}(x)}{\partial x}$  (here  $\epsilon$  is a cutoff). The bosonic field has a decomposition

$$\varphi_{j\alpha}(x) = \varphi_{j\alpha}^0 + \alpha N_{j\alpha} 2\pi x/L + \bar{\varphi}_{j\alpha}(x), \quad (\text{A2})$$

where the number operator  $N_{j\alpha}$  and its conjugate  $\varphi_{j\alpha}^0$  satisfy the commutation relations

$$[N_{j\alpha}, \varphi_{l\beta}^0] = i\delta_{jl}\delta_{\alpha\beta}, \quad (\text{A3})$$

and the periodic fields  $\bar{\varphi}_{j\alpha}(x) = \bar{\varphi}_{j\alpha}(x + L)$  have the usual form,

$$\bar{\varphi}_{j\alpha}(x) = \sum_q \theta(q\alpha) \sqrt{\frac{2\pi}{L|q|}} e^{-|q|\epsilon/2} \left( e^{iqx} a_{qj} + e^{-iqx} a_{qj}^\dagger \right), \quad (\text{A4})$$

with  $a_{qj}$  and  $a_{qj}^\dagger$  satisfying standard boson commutation relations [ $\theta(x)$  is the step function]. The boundary condition for the fermion fields,  $\psi_{j\alpha}(x+L) = (-1)^{N_j} \psi_{j\alpha}(x)$ , depends on the parity of the number of particles,  $N_j = 2N_{j\alpha}$ . The Hamiltonian  $H = H_0 + H_{int}$  is quadratic in boson fields:

$$H_0 = \sum_{j\alpha} \frac{v_j}{4\pi} \int_0^L dx \left[ \frac{\partial \varphi_{j\alpha}(x)}{\partial x} \right]^2, \quad (\text{A5})$$

and

$$H_{int} = \frac{1}{2} \sum_{jl} \int_0^L dx \int_0^L dy \left[ \sum_{\alpha} \frac{\alpha}{2\pi} \frac{\partial \varphi_{j\alpha}(x)}{\partial x} \right] U_{jl}(x-y) \times \left[ \sum_{\beta} \frac{\beta}{2\pi} \frac{\partial \varphi_{l\beta}(y)}{\partial y} \right], \quad (\text{A6})$$

where  $U_{jl}(x)$  is the screened potential. Using Eqs. (A2) and (A4), and after separating out the zero-mode part of the Hamiltonian,  $H^0$ , from the bosonic part,  $\bar{H}$ , the total Hamiltonian  $H = H^0 + \bar{H}$  can be written as

$$H = \frac{\pi}{L} \sum_{j\alpha\beta} N_{j\alpha} \left( v_j \delta_{jl} \delta_{\alpha\beta} + \frac{u_{jl}}{2} \right) N_{l\beta} + \sum_{qjl} e^{-|q|\epsilon} |q| \left[ v_j \delta_{jl} a_{qj}^\dagger a_{qj} + \frac{u_{jl}}{4} (a_{qj}^\dagger + a_{-qj})(a_{-ql}^\dagger + a_{ql}) \right], \quad (\text{A7})$$

where  $u_{jl} = \pi^{-1} \int dx U_{jl}(x)$ .

In order to calculate correlation functions, the Hamiltonian  $\bar{H}$ , corresponding to the second term of (A7), has to be brought to the canonical form. This is done in two steps. First, we perform a two-component Bogolubov's transformation in order to eliminate the cross-terms with opposite momenta,

$$a_{qj} = \sum_l (X_{jl} b_{ql} + Y_{jl} b_{-ql}^\dagger), \quad \sum_l (X_{jl} X_{ln}^\dagger - Y_{jl} Y_{ln}^\dagger) = \delta_{jn}. \quad (\text{A8})$$

We then obtain

$$\bar{H} = \sum_{qjl} e^{-|q|\epsilon} |q| b_{qj}^\dagger (X^\dagger - Y^\dagger)_{jl} v_l (X - Y)_{ln} b_{qn}, \quad (\text{A9})$$

where the matrices  $X$  and  $Y$  must satisfy

$$\sum_{lm} (X^\dagger + Y^\dagger)_{jl} (u_{lm} + v_l \delta_{lm}) (X + Y)_{mn} = \sum_l (X^\dagger - Y^\dagger)_{jl} v_l (X - Y)_{ln}. \quad (\text{A10})$$

Second, we diagonalize the Hamiltonian (A9) by first presenting the matrices  $X$  and  $Y$  as

$$X = \cosh \lambda O, \quad Y = \sinh \lambda O, \quad (\text{A11})$$

where  $\lambda_{jl} = \lambda_j \delta_{jl}$  is diagonal matrix of Bogolubov's angles  $\lambda_j$  and  $O$  is an orthogonal matrix, and then by introducing new boson operators  $c_{qj} = \sum_l O_{jl} b_{ql}$ . The Hamiltonian  $\bar{H}$  then takes the form

$$\bar{H} = \sum_{qj} e^{-|q|\epsilon} |q| \tilde{v}_j c_{qj}^\dagger c_{qj}, \quad (\text{A12})$$

with renormalized Fermi velocities  $\tilde{v}_j = e^{-2\lambda_j} v_j$ . The old and new boson operators are related as

$$a_{qj} = \cosh \lambda_j c_{qj} + \sinh \lambda_j c_{-qj}^\dagger. \quad (\text{A13})$$

Using the decomposition (A11), Eq. (A10) takes the form  $\tilde{O}AO = 0$ , where  $\tilde{O}$  is the transposed matrix, and the matrix  $A$  is given by

$$A_{jl} = u_{jl} e^{\lambda_j + \lambda_l} + \delta_{jl} v_j (e^{2\lambda_j} - e^{-2\lambda_j}). \quad (\text{A14})$$

The Bogolubov's angles  $\lambda_j$  are found from the condition that all the eigenvalues of  $A_{jl}$  vanish. In the two-component case, this yields

$$e^{-2\lambda_1} = \sqrt{Q \frac{v_1 + u_{11} - v_2 Q}{v_1 Q - v_2 - u_{22}}}, \quad e^{-2\lambda_2} = Q/e^{-2\lambda_1},$$

$$Q = \sqrt{\left(1 + \frac{u_{11}}{v_1}\right) \left(1 + \frac{u_{22}}{v_2}\right) - \frac{u_{12}^2}{v_1 v_2}}. \quad (\text{A15})$$

The Luttinger liquid interaction parameter is given by  $\mu_j = \sinh^2 \lambda_j$ . In the case of weak interactions,  $u_{jl}/v_j \ll 1$ , we have  $\lambda_j \simeq -u_{jj}/4v_j$  so that  $\mu_j \simeq \lambda_j^2 \simeq (u_{jj}/4v_j)^2$  and  $\tilde{\Delta}_j \simeq \Delta_j(1 + u_{jj}/2v_j)$ .

With the Hamiltonian (A12), the time-dependence of new operators is standard,  $c_{qj}(t) = e^{-i\tilde{v}_j |q| t} c_{qj}$ . Using the relation (A13), the periodic fields (A4) take the form

$$\bar{\varphi}_{j\alpha}(x, t) = \sum_q \sqrt{\frac{2\pi}{L|q|}} e^{-|q|\epsilon/2}$$

$$\times \left[ \theta(q\alpha) \cosh \lambda_j + \theta(-q\alpha) \sinh \lambda_j \right]$$

$$\times \left( e^{iqx - i\tilde{v}_j |q| t} c_{qj} + e^{-iqx + i\tilde{v}_j |q| t} c_{qj}^\dagger \right). \quad (\text{A16})$$

The time-dependence of zero-modes is governed by the zero-mode part (first term) of the Hamiltonian (A7). The time-dependent bosonic field is finally obtained as

$$\varphi_{j\alpha}(x, t) = \varphi_{j\alpha}^0 + \alpha N_{j\alpha} 2\pi(x - \alpha v_j t)/L$$

$$- \sum_{l\beta} u_{jl} N_{l\beta} \pi t/L + \bar{\varphi}_{j\alpha}(x, t). \quad (\text{A17})$$

We are now in position to calculate the Green functions. For this, we separate out annihilation and creation parts of the periodic field (A16),  $\bar{\varphi}_{j\alpha}(x, t) = \bar{\varphi}_{j\alpha}^-(x, t) +$

$\bar{\varphi}_{j\alpha}^+(x, t)$ , which satisfy the following commutation relations

$$[\bar{\varphi}_{j\alpha}^-(x, t), \bar{\varphi}_{j\alpha}^+(x', t')] = \ln f_\alpha(z_{j\alpha} - z'_{j\alpha})$$

$$+ \mu_j \ln \left[ f_\alpha(z_{j\alpha} - z'_{j\alpha}) f_{-\alpha}(z_{j,-\alpha} - z'_{j,-\alpha}) \right], \quad (\text{A18})$$

with  $z_{j\alpha} = x - \alpha \tilde{v}_j t$ . Then we present the fermion operator (A1) in the normal-ordered form,

$$\psi_{j\alpha}(x, t) = \psi_{j\alpha}^0(x, t) \bar{\psi}_{j\alpha}(x, t),$$

$$\psi_{j\alpha}^0(x, t) = e^{iv_j(1+u_{jj}/2)\pi t/L} e^{i\varphi_{j\alpha}^0}$$

$$\times e^{i\alpha N_{j\alpha} 2\pi z_{j\alpha}/L - i \sum_{l\beta} u_{jl} N_{l\beta} \pi t/L},$$

$$\bar{\psi}_{j\alpha}(x, t) = L^{-1/2} \left( 2\pi\epsilon/L \right)^{\mu_j} e^{i\bar{\varphi}_{j\alpha}^+(x, t)} e^{i\bar{\varphi}_{j\alpha}^-(x, t)}, \quad (\text{A19})$$

where we again separated out zero-mode and periodic parts. Using Eq. (A19) together with commutators (A3) and (A18), the Green function (5) can be straightforwardly calculated as

$$D_\alpha(x, t) = \left( \frac{2\pi\epsilon}{L} \right)^{2(\mu_2 + \mu_2)} \frac{e^{-it\delta_P - it\delta_u}}{L^2}$$

$$\times \left[ f_\alpha(z_{1\alpha}) \right]^{1+\mu_1} \left[ f_{-\alpha}(z_{1,-\alpha}) \right]^{\mu_1}$$

$$\times \left[ f_{-\alpha}(z_{2,-\alpha}) \right]^{1+\mu_2} \left[ f_\alpha(z_{2\alpha}) \right]^{\mu_2}, \quad (\text{A20})$$

where  $\delta_P = \pi(v_1 + v_2)/L$  and  $\delta_u = \pi(u_{11} + u_{22} + 2u_{12})/2$  are the energy shifts due the changes in the parity of electron and hole numbers and in the Coulomb energy, caused by a removal of an  $e$ - $h$  pair. We assume that the screened interaction is the same for electrons and holes,  $u_{11} = u_{22} = -u_{12} = u$ , so that  $\delta_u = 0$ . Then, after absorbing the factor  $2\pi/L$  into  $\epsilon$ , we arrive at Eq. (6).

Note finally that the above calculation is easily generalized if the ring is penetrated by a magnetic flux  $\phi$ . In this case, the electron and hole number operators should be shifted by flux-dependent constants,  $N_{1\alpha} \rightarrow N_{1\alpha} + \alpha\phi/\phi_0$  and  $N_{2\alpha} \rightarrow N_{2\alpha} - \alpha\phi/\phi_0$ , where  $\phi_0$  is the flux quantum. This results in a replacement  $\delta_P \rightarrow \delta_P(1 - 2\alpha\phi/\phi_0)$  in Eq. (6).

## APPENDIX B:

Substituting the Fourier expansion

$$\left[ f_\alpha(z_{j\alpha}) \right]^\nu = \sum_n b_\nu(n) e^{i\alpha 2\pi n z_{j\alpha}/L},$$

$$b_\nu(n) = \frac{\sin \pi\nu}{\pi} B(n + \nu, 1 - \nu), \quad (\text{B1})$$

into Eq. (6),  $D_\alpha(\omega)$  takes the form

$$D_\pm(\omega) = \epsilon^{2(\mu_1 + \mu_2)} \sum_{\{n\}} b_{1+\mu_1}(n_1) b_{\mu_1}(n'_1) b_{1+\mu_2}(n_2)$$

$$\times b_{\mu_2}(n'_2) \Lambda_\pm(\omega, \{n\}), \quad (\text{B2})$$

with

$$\begin{aligned}\Lambda_{\pm}(\omega, \{n\}) &= \frac{1}{L^2} \int dt \int_0^L dx \exp \left[ -i\omega t \right. \\ &\quad \left. \pm i \frac{2\pi}{L} \left( n_1 z_{1\pm} - n'_1 z_{1\mp} - n_2 z_{2\mp} + n'_2 z_{2\pm} \right) \right] \\ &= \frac{2\pi}{L} \delta_{n_1 - n'_1, n_2 - n'_2} \delta \left[ \omega + \frac{2\pi \tilde{v}_1}{L} (n_1 + n'_1) \right. \\ &\quad \left. + \frac{2\pi \tilde{v}_2}{L} (n_2 + n'_2) \right], \quad (\text{B3})\end{aligned}$$

where we absorbed the parity shift  $\delta_P$  into  $\omega$ . The Kronecker delta and the delta-function reflect the conservation of momentum and energy, respectively. Thus, we obtain

$$D_{\alpha}(\omega) = \frac{2\pi}{L} \sum_{mn} C_{mn} \delta(\omega + \tilde{\Delta}_1 m + \tilde{\Delta}_2 n), \quad (\text{B4})$$

with

$$\begin{aligned}C_{mn} &= \epsilon^{2(\mu_1 + \mu_2)} \sum_l b_{1+\mu_1}[(m+n)/2 - l] b_{1+\mu_2}(n-l) \\ &\quad \times b_{\mu_1}[(m-n)/2 + l] b_{\mu_2}(l). \quad (\text{B5})\end{aligned}$$

Finally, using the integral representation for the Beta-function in Eq. (B1) we arrive at Eq. (11). The sum in Eq. (B4) is constrained by the selection rule that  $m$  and  $n$  are of the same parity, as can be seen from Eq. (B3). From Eq. (B4), the emission spectrum (2) follows.

### APPENDIX C:

Here we consider the case when the level spacings in the conduction and valence bands are commensurate:  $\tilde{\Delta}_1/\tilde{\Delta}_2 = p/q$ , where  $p$  and  $q$  are integers. Then Eq. (B4) takes the form

$$\begin{aligned}D_{\alpha}(\omega) &= \frac{2\pi}{L} \sum_{mn} C_{mn} \delta \left( \omega + \tilde{\Delta} \frac{mp + nq}{p + q} \right) \\ &= \frac{2\pi}{L} \sum_k C_k \delta(\omega + \tilde{\Delta} k/Q), \quad (\text{C1})\end{aligned}$$

where  $Q = p + q$ ,  $P = p - q$ ,  $\tilde{\Delta} = \tilde{\Delta}_1 + \tilde{\Delta}_2$ , and

$$\begin{aligned}C_k &= \sum_{mn} \delta_{k, mp+nq} C_{mn} = \sum_{MN} \delta_{k, MP+NQ} C_{N+M, N-M} \\ &= \sum_{MN} \delta_{k-MP, NQ} C_{\frac{k}{Q}+M(1-\frac{P}{Q}), \frac{k}{Q}-M(1+\frac{P}{Q})}. \quad (\text{C2})\end{aligned}$$

Using the relation

$$\sum_N \delta_{k, NQ} = \frac{1}{Q} \sum_{l=0}^{Q-1} e^{-i2\pi lk/Q}, \quad (\text{C3})$$

the oscillator strengths can be presented as

$$C_k = \frac{1}{Q} \sum_{l=0}^{Q-1} e^{-i2\pi lk/Q} f_l(k), \quad (\text{C4})$$

with

$$f_l(k) = \sum_M e^{i2\pi lMP/Q} C_{\frac{k}{Q}+M(1-\frac{P}{Q}), \frac{k}{Q}-M(1+\frac{P}{Q})}. \quad (\text{C5})$$

Using integral representation (11), the sum over  $M$  can be explicitly performed. For  $k/Q = |\omega|/\tilde{\Delta} \gg 1$ , the resulting expression for coefficients  $f_l$  takes the form

$$\begin{aligned}f_l(k) &= \int_{-\infty}^{\infty} \frac{d\phi_1 d\phi_2}{(2\pi)^2} \frac{\epsilon^{2(\mu_1 + \mu_2)} e^{-i(\phi_1 + \phi_2)k/Q}}{(-i\phi_1)^{1+\mu_1} (-i\phi_2)^{1+\mu_2}} \\ &\quad \times \frac{1}{\left(1 - s_l - i s_l [\phi_2 + (\phi_1 + \phi_2)P/Q]\right)^{\mu_1}} \\ &\quad \times \frac{1}{\left(1 - s_l^* - i s_l^* [\phi_1 - (\phi_1 + \phi_2)P/Q]\right)^{\mu_2}}, \quad (\text{C6})\end{aligned}$$

where  $s_l = e^{i2\pi lP/Q}$ . The  $l$ -dependence of  $f_l(k)$  is determined by the relative magnitude of  $Q/k$  and  $|1 - s_l|$ :

$$f_l(k) \simeq \left| \frac{\epsilon k}{Q} \right|^{2(\mu_1 + \mu_2)} \quad (\text{C7})$$

for  $k/Q \ll |1 - s_l|^{-1}$ , and

$$f_l(k) \simeq \left( \frac{\epsilon^2 k/Q}{1 - s_l} \right)^{\mu_1} \left( \frac{\epsilon^2 k/Q}{1 - s_l^*} \right)^{\mu_2} \quad (\text{C8})$$

for  $k/Q \gg |1 - s_l|^{-1}$ , with the two estimates matching at  $k/Q \sim |1 - s_l|^{-1}$ .

In the case  $\tilde{\Delta}_1/\tilde{\Delta}_2 = 3$ , corresponding to  $P = 2$  and  $Q = 4$  so that  $s_l = (-1)^l$ , the coefficients  $f_l$  take two different values depending on the parity of  $l$ ,

$$f_{\text{even}}(k) \simeq \left| \frac{\epsilon k}{4} \right|^{2(\mu_1 + \mu_2)} = \left| \frac{\epsilon \omega}{\tilde{\Delta}} \right|^{2(\mu_1 + \mu_2)}, \quad (\text{C9})$$

$$f_{\text{odd}}(k) \simeq \left| \frac{\epsilon^2 k}{8} \right|^{\mu_1 + \mu_2} = \left| \frac{\epsilon^2 \omega}{2\tilde{\Delta}} \right|^{\mu_1 + \mu_2}, \quad (\text{C10})$$

yielding

$$C_k = \left| \frac{\epsilon \omega}{\tilde{\Delta}} \right|^{2\mu} \frac{1 + (-1)^k}{2} \frac{1 + e^{i\pi k/2} \left| \frac{2\omega}{\tilde{\Delta}} \right|^{-\mu}}{2} \quad (\text{C11})$$

with  $\mu = \mu_1 + \mu_2$ . Obviously,  $C_k = 0$  for  $k$  odd. For  $k$  even, we have

$$C_{4l} \simeq \left| \frac{\epsilon \omega}{\tilde{\Delta}} \right|^{2\mu} \frac{1 + \left| \frac{2\omega}{\tilde{\Delta}} \right|^{-\mu}}{2}, \quad (\text{C12})$$

$$C_{4l+2} \simeq \left| \frac{\epsilon \omega}{\tilde{\Delta}} \right|^{2\mu} \frac{1 - \left| \frac{2\omega}{\tilde{\Delta}} \right|^{-\mu}}{2}, \quad (\text{C13})$$

leading to Eq. (18).

\*On leave from Vanderbilt University

- <sup>1</sup> K. Brunner, U. Bockelmann, G. Abstreiter, M. Walther, G. Bohm, G. Trankle, and G. Weimann Phys. Rev. Lett. **69**, 3216 (1992).
- <sup>2</sup> J.-Y. Marzin, J.-M. Gérard, A. Izraël, D. Barrier, and G. Bastard, Phys. Rev. Lett. **73**, 716 (1994).
- <sup>3</sup> A. Zrenner, J. Chem. Phys. **112**, 7790 (2000).
- <sup>4</sup> D. Gammon, Nature **405** 899 (2000).
- <sup>5</sup> R. J. Warburton, C. Schäfflein, D. Haft, F. Bicken, A. Lorke, K. Karrai, J. M. Garcia, W. Schoenfeld, and P. M. Petroff, Nature **405**, 926 (2000).
- <sup>6</sup> D. V. Regelman, E. Dekel, D. Gershoni, E. Ehrenfreund, A. J. Williamson, J. Shamway, A. Zunger, W. V. Schoenfeld, and P. M. Petroff, ArXiv: cond-mat 0105589.
- <sup>7</sup> M. Ikezawa, Y. Masumoto, T. Takagahara, and S. V. Nair, Phys. Rev. Lett. **79**, 3522 (1997).
- <sup>8</sup> L. Landin M. S. Miller, M.-E. Pistol, C. E. Pryor, and L. Samuelson, Science **280**, 262 (1998).
- <sup>9</sup> M. Bayer, T. Gutbrod, A. Forchel, V. D. Kulakovskii, A. Gorbunov, M. Michel, R. Steffen, and K. H. Wang, Phys. Rev. B **58**, 4740 (1998).
- <sup>10</sup> V. D. Kulakovskii, G. Bacher, R. Weigand, T. Kummell, A. Forchel, E. Borovitskaya, K. Leonardi, and D. Hommel, Phys. Rev. Lett. **82**, 1780 (1999).
- <sup>11</sup> E. Dekel, D. Gershoni, E. Ehrenfreund, D. Spektor, J. M. Garcia, and P. M. Petroff, Phys. Rev. Lett. **80**, 4991 (1998).
- <sup>12</sup> E. Dekel, D. Gershoni, E. Ehrenfreund, J. M. Garcia, and P. M. Petroff, Phys. Rev. B **61**, 11009 (2000).
- <sup>13</sup> E. Dekel, D. Regelman, D. Gershoni, E. Ehrenfreund, W. V. Schoenfeld, and P. M. Petroff, Phys. Rev. B **62**, 11038 (2000).
- <sup>14</sup> E. Dekel, D. Regelman, D. Gershoni, E. Ehrenfreund, W. V. Schoenfeld, and P. M. Petroff, Solid State Commun. **117**, 395 (2001).
- <sup>15</sup> F. Findeis, A. Zrenner, G. Bohm, and G. Abstreiter, Solid State Commun. **114**, 227 (2000).
- <sup>16</sup> M. Bayer, O. Stern, P. Hawrylak, S. Fafard, and A. Forchel, Nature **405**, 923 (2000).
- <sup>17</sup> P. Hawrylak, Phys. Rev. B **60**, 5597 (1999).
- <sup>18</sup> Y. Toda, O. Moriwaki, M. Nishioka, and Y. Arakawa, Phys. Rev. Lett. **82**, 4114 (1999).
- <sup>19</sup> A. Lorke, R. J. Luyken, A. O. Govorov, J. P. Kotthaus, J. M. Garcia, and P. M. Petroff, Phys. Phys. Lett. **84**, 2223 (2000).
- <sup>20</sup> H. Pettersson R. J. Warburton, A. Lorke, K. Karrai, J. P. Kotthaus, J. M. Garcia, and P. M. Petroff, Physica E **6**, 510 (2000).
- <sup>21</sup> A. Chaplik, Pis'ma Zh. Eksp. Teor. Fiz. **62**, 885 (1995) [JETP Lett. **62**, 900 (1995)].
- <sup>22</sup> R. A. Römer and M. E. Raikh, Phys. Rev. B **62**, 7045 (2000).
- <sup>23</sup> H. Hu, D.-J. Li, J.-L. Zhu, and J.-J. Xiong, J. Phys. Condens. Matter **12**, 9145 (2000).
- <sup>24</sup> H. Hu, G.-M. Zhang, J.-L. Zhu, and J.-J. Xiong, Phys. Rev. B **63**, 045320 (2001).
- <sup>25</sup> H. Hu, J.-L. Zhu, D.-J. Li, and J.-J. Xiong, Phys. Rev. B **63**, 195307 (2001).
- <sup>26</sup> J. Song and S. E. Ulloa, Phys. Rev. B **63**, 125302 (2001).
- <sup>27</sup> See, e.g., H. J. Schulz, in *Proceedings of Les Houches Summer School LXI*, edited by E. Akkermans, G. Montambaux, J. Pichard, and J. Zinn-Justin, (Elsevier, Amsterdam, 1995), p. 533.
- <sup>28</sup> A. O. Gogolin, Phys. Rev. Lett. **71**, 2995 (1993).
- <sup>29</sup> N. V. Prokof'ev, Phys. Rev. B **49**, 2148 (1994).
- <sup>30</sup> C. L. Kane, K. A. Matveev, and L. I. Glazman, Phys. Rev. B **49**, 2253 (1994).
- <sup>31</sup> M. Sassetti and B. Kramer, Phys. Phys. Lett. **80**, 1485 (1998).
- <sup>32</sup> B. Kramer and M. Sassetti, Phys. Phys. B **62**, 4238 (2000).
- <sup>33</sup> I. E. Dzyaloshinsky and A. I. Larkin, Zh. Eksp. Teor. Fiz. **65**, 411 (1974) [Sov. Phys. JETP **38**, 202 (1974)].
- <sup>34</sup> K. A. Matveev and L. I. Glazman, Phys. Rev. Lett. **70**, 990 (1993).
- <sup>35</sup> K. Penc and J. Sólyom, Phys. Rev. B **47**, 6273 (1993).
- <sup>36</sup> T. V. Shahbazyan and S. E. Ulloa, Phys. Rev. B **55**, 13702 (1997).
- <sup>37</sup> O. M. Auslaender, A. Yacoby, R. de Picciotto, K. W. Baldwin, L. N. Pfeiffer, K. W. West, Phys. Rev. Lett. **84**, 1764 (2000).
- <sup>38</sup> T. Kleimann, M. Sassetti, B. Kramer, and A. Yacoby, Phys. Rev. B **62**, 8144 (2000).
- <sup>39</sup> B. L. Altshuler, Y. Gefen, A. Kamenev, and L. S. Levitov, Phys. Rev. Lett. **78**, 2803 (1997).

FIG. 1. Emission spectrum for  $\tilde{\Delta}_1 = 3\tilde{\Delta}_2$ . In the low-frequency domain, the single-particle peaks acquire weak many-body satellites; in the high-frequency domain, the heights of the single-particle ( $|\omega|/\tilde{\Delta} = l$ ) and many-body ( $|\omega|/\tilde{\Delta} = l + 1/2$ ) peaks are close to each other. Inset: Single-particle spectra of electrons and hole in conduction and valence bands, respectively;  $\omega_{th}$  is the energy distance between the corresponding Fermi levels.

FIG. 2. The distribution function Eq. (20) of the peak heights within the interval  $\tilde{\Delta}$  is plotted schematically versus  $x = C/C_0$ . The minimal value of  $x$  is  $x_{min} \sim 1$ , while  $x_{max} \sim |\omega/\tilde{\Delta}|^{1-\mu} \gg 1$ . The point  $x = \mu^{-1}$  corresponds to the average oscillator strength.



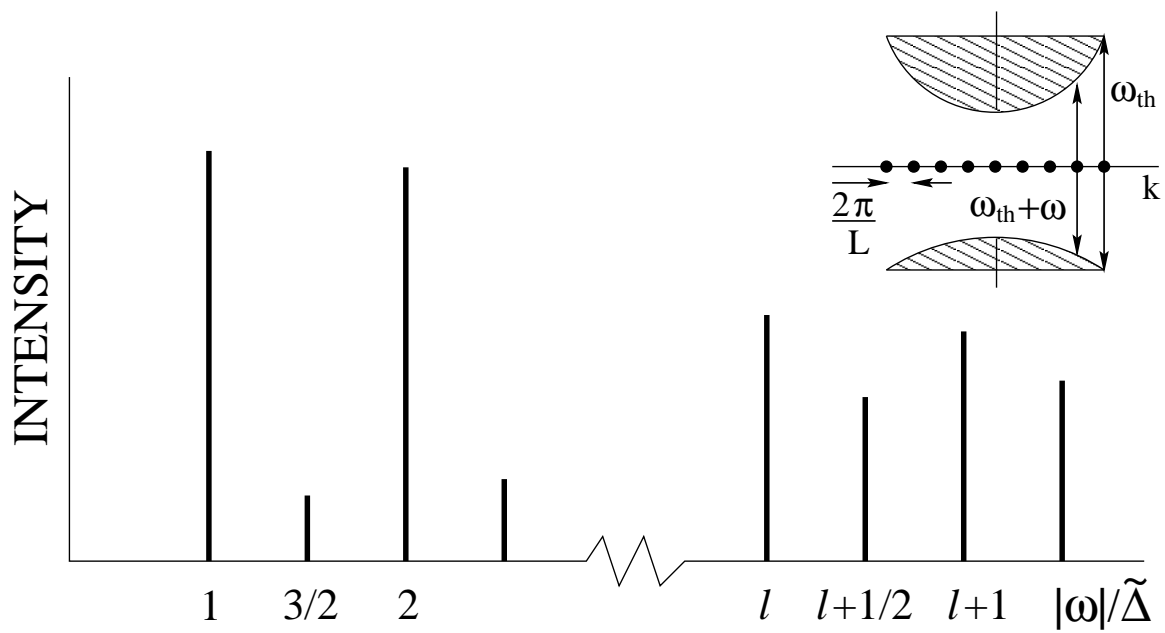


Fig. 1

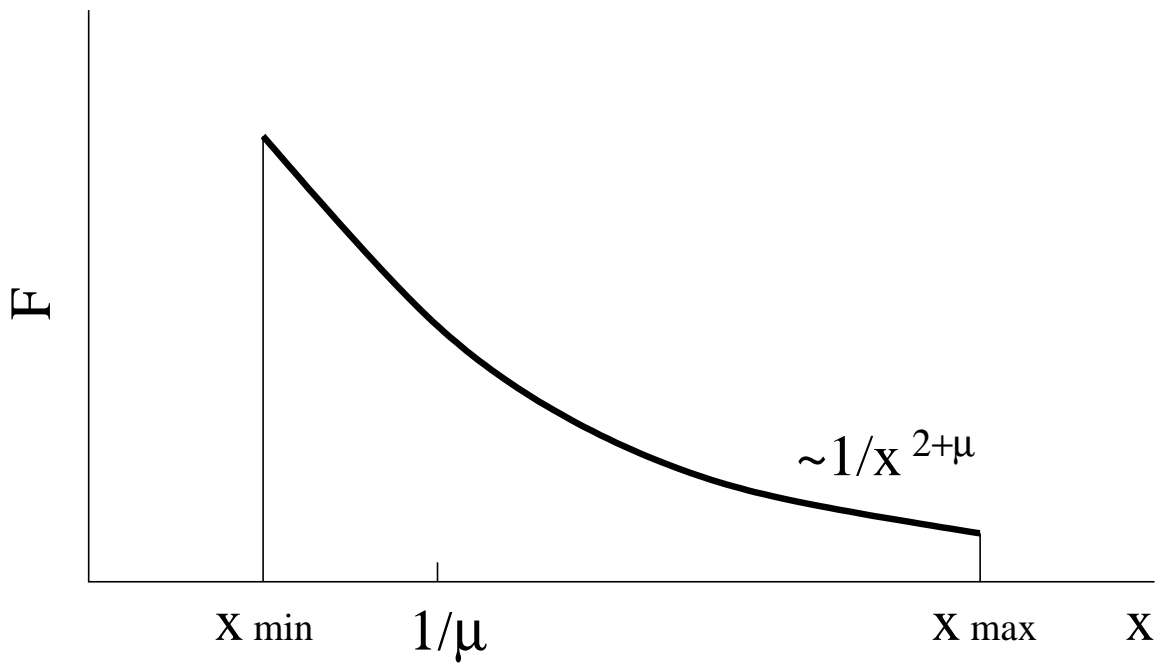


Fig. 2